JOURNAL OF MATERIALS SCIENCE 23 (1988) 3413–3419

Influence of powder characteristics on gas pressure sintering of Si_3N_4

M. MITOMO, N. YANG*, Y. KISHI‡, Y. BANDO
National Institute for Research in Inorganic Materials, Namiki 1-1, Sakura-mura, Niihari-gun, Ibaraki, Japan

The sintering behaviours of four kinds of Si_3N_4 powders were investigated by dilatometry in 10 atm N_2 at 1890, 1930 and 2050° C. The sinterabilities of powders were compared and discussed in relation to the powder characteristics. A large size distribution in the powder accelerated grain and pore growth at <1800° C, which resulted in the inhibition of further densification at >1800° C. The presence of carbon in a powder prevented densification. A powder with a uniform grain size kept the microstructure of the sintered material uniform during sintering at <1800° C and gave a high degree of shrinkage at >1800° C. Densification at >1800° C was accompanied by the dissolution of equi-axial β-Si_3N_4 grains and reprecipitation as elongated β-Si_3N_4 grains from the oxynitride liquid. The relation between the densification and microstructure is discussed in terms of the relative rates of densification and grain growth.

1. Introduction

It is known that the powder characteristics have a large influence on the sintering behaviour of Si_3N_4. Wötting and Ziegler [1] pointed out that the degree of densification in pressureless sintering depended largely on the particle size, oxygen and carbon content. Homma *et al.* [2] reported that the specific surface area and α-content had a large influence on the density of sintered materials. Bellosi *et al.* [3] showed that a fine particle size was necessary to get high-density materials. To fabricate high-density materials by pressureless sintering [2, 4], larger amounts of additive's were necessary than for hot-pressing [5]. The influence of the powder characteristics on densification was masked when large amounts of additives were employed [1].

Gas pressure sintering has enabled sintering to be carried out at a higher temperature than hot-pressing or pressureless sintering by stabilizing Si_3N_4 in a high nitrogen pressure [6, 7]. Therefore, the amounts of additives could be reduced to the same level as in hot-pressing. The results on sintering behaviour in 10 atm N_2 revealed that densification occurred at about 1400, 1700 and 1900° C. The first two processes were rearrangement and solution–reprecipitation of liquid-phase sintering. The processes were basically the same as in pressureless sintering. The α to β phase transition took place during the solution–reprecipitation process. The contribution of the process was large enough to get nearly fully dense materials when a large amount of additive was used. In gas pressure sintering, additional densification took place at about 1900° C when small amounts of additive were used. The densification at about 1900° C was also a solution–reprecipitation process accompanied by the solution of equi-axial β-Si_3N_4 grains and reprecipitation as needle-like β-Si_3N_4 grains [7]. It has been shown [8] that the strength and fracture toughness of ceramics are determined by the microstructure and fracture behaviour. The relation between the powder characteristics, densification behaviour and microstructure development during gas pressure sintering is not well understood.

In the present work, the densification behaviours of four kinds of powder were investigated using a dilatometer in 10 atm N_2. The differences in the densification behaviour, density and microstructure of sintered materials were investigated in relation to the powder characteristics. The properties of a desirable starting powder for gas pressure sintering were also investigated.

2. Experimental procedure

2.1. Starting materials

Four kinds of Si_3N_4 powder were mixed with 5 wt % Y_2O_3 and 2 wt % Al_2O_3. They were made by different preparation methods. Powder A was prepared by the nitridation of silicon (Starck, W. Germany, LC-10 grade). Powder B was made by the chemical vapour deposition method (GTE Sylvania, USA, SN-502 grade). Powder C was made by carbothermal reduction and nitridation of silica (Toshiba Ceramics Co., Japan). Powder D was made by thermal decomposition of

Present address: Materials Research Laboratory, Industrial Technology Research Institute, 195-5 Chung-hsing Rd, Chutung, Hsinchu 31015, Taiwan.
‡*Present address*: Central Research Laboratory, Nihon Cement Co., 1-2-3 Kiyosumi, Kohtoh-ku, Tokyo, Japan.

0022–2461/88 $03.00 + .12

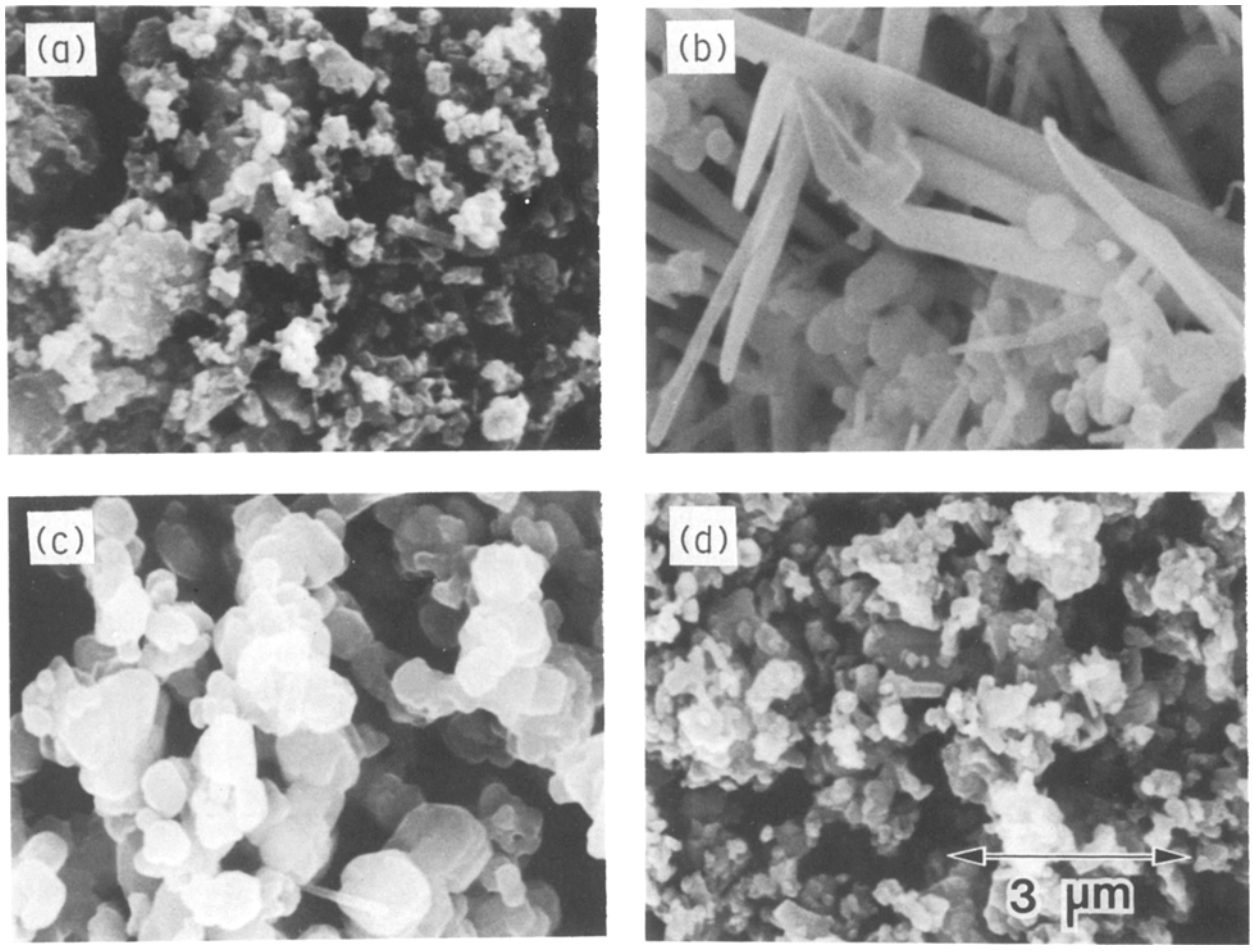

Figure 1 SEM micrographs of starting powders (see Table I): (a) A, (b) B, (c) C and (d) D.

$Si(NH)_2$ which was prepared by the reaction of $SiCl_4$ and NH_3 at low temperature (Toyo Soda Co., Japan, TS-7 grade). The characteristics of the powders are compared in Table I. The average grain size was determined as that corresponding to 50% cumulative weight in the size distribution curve. The grain shapes of the powders are shown in Fig. 1. Powder B is composed of both spherical and needle-like grains. The other powders are composed of spherical grains. The size distribution was the most narrow in Powder C, as can be seen in the figure. The oxygen and carbon contents were the highest in Powder C. The amount of metallic impurities was the highest in Powder A.

2.2. Sintering

The Si_3N_4 powder and additives were mixed by ball-milling in n-hexane for 3 h using Si_3N_4 balls and pot. After drying, about 3 g of the mixture was compressed in a steel die with an inner diameter of 16 mm under 19.6 MPa. The compact was then pressed isostatically under 196 MPa. The compact was heated at a constant heating rate of 15° C min^{-1} and then kept at 1890, 1930 or 2050° C for 1 h in 10 atm N_2. The densification curve was measured using a dilatometer [7].

2.3. Microstructural observations

The microstructures of sintered materials were observed with a scanning electron microscope (SEM). The difference in the composition of the grain-boundary glassy phase with difference of sintering temperature was investigated with Powder D using a 400 kV analytical electron microscope (STEM). The material obtained by hot-pressing at 1700° C was an example of material fabricated at low temperature. Hot-pressing was necessary to get high-density materials. Gas pressure-sintered material obtained

TABLE I Characteristics of starting Si_3N_4 powders

Powder	Particle size (μm)		Specific surface area ($m^2 g^{-1}$)	Impurities*			Phase ratio $\alpha/(\alpha + \beta)$ (%)
	Range	Average		O (wt %)	C (wt %)	Total metals (p.p.m.)	
A	0.05 to 5.0	0.5	15	1.4	0.1	1300	94
B	0.1 to 5.0	1.3	4	1.5		240	95†
C	0.2 to 1.0	1.2	5	2.0	1.1	130	95
D	0.05 to 1.0	0.6	12	1.0	0.1	70	87

*Data were supplied from manufacturers.
†About 40% of the powder is amorphous.

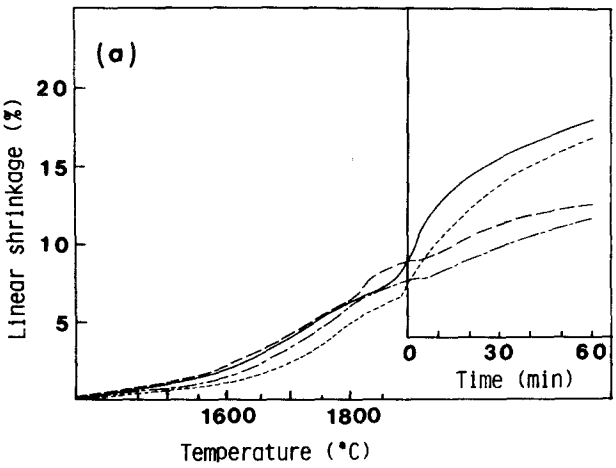

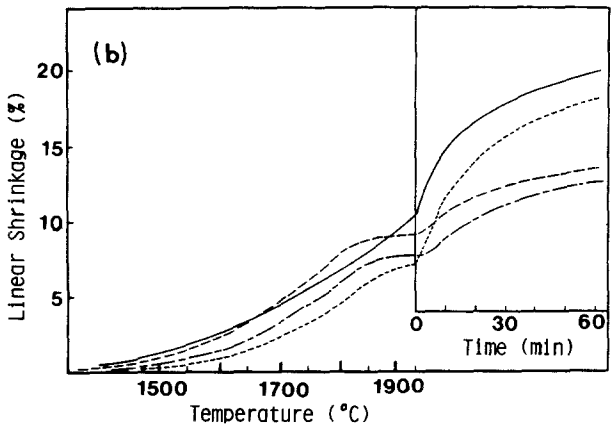

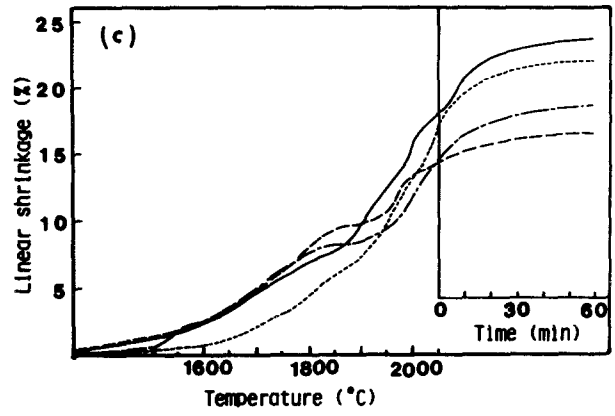

Figure 2 Linear shrinkage during heating at 15° C min^{-1} and keeping at (a) 1890, (b) 1930 and (c) 2050° C. Powder (– – –) A, (- - - - -) B, (– – –) C, (——) D.

at 1930° C in 10 atm N_2 was used as a specimen fabricated at high temperature.

3. Results and discussion

The linear shrinkage during heating-up and keeping at given temperatures is shown in Fig. 2 for each powder. The highest shrinkage is obtained with Powder D. The lowest shrinkage is with Powder C at 1890 and 1930° C, and Powder A at 2050° C. The shrinkage rates are plotted in Fig. 3. It must be noted that the difference in the densification behaviour during gas pressure sintering at $< 1800°$ C is smaller than that at $> 1800°$ C. This means that the difference in the densification behaviour with the difference of powder characteristics is attributed to that at high temperature. The densification rate is higher with Powders B and D than with Powders A and C at $> 1800°$ C.

Nearly fully dense materials could be fabricated with large amounts of additives in pressureless sintering at $< 1800°$ C. It is known that the powder characteristics influence the densification behaviour very much when Si_3N_4 is sintered in 1 atm N_2. A phase change from α to β has been observed [2] during

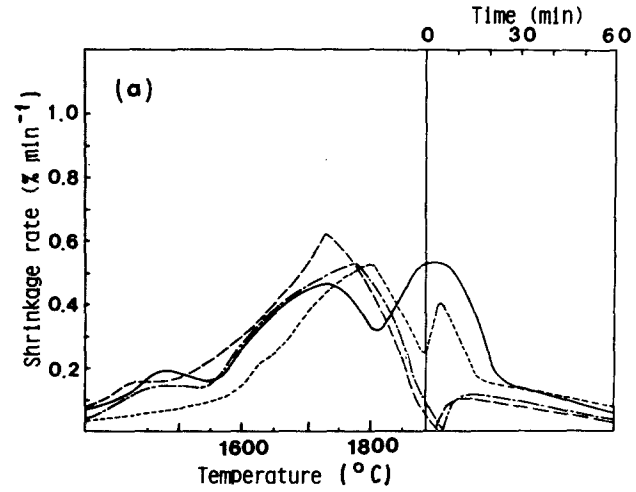

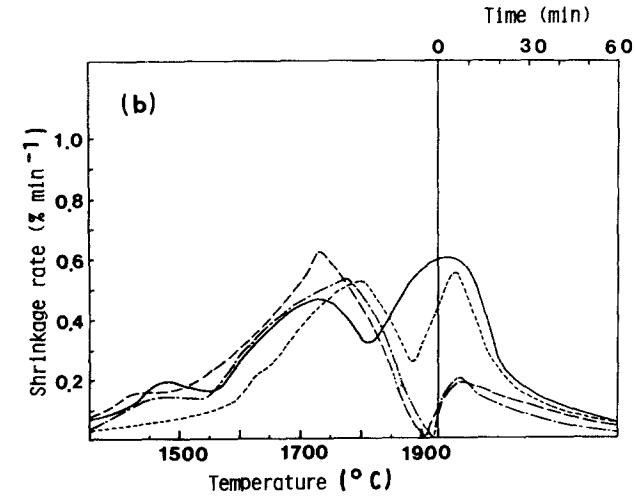

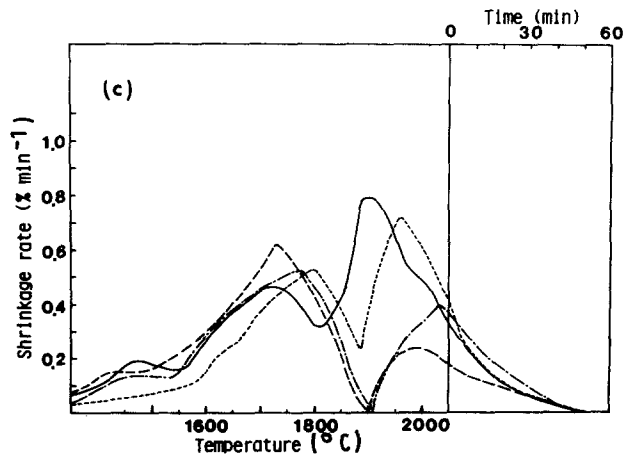

Figure 3 Shrinkage rate during heating at 15° C min^{-1} and keeping at (a) 1890, (b) 1930 and (c) 2050° C. Powder (– – –) A, (- - - - -) B, (– – –) C, (——) D.

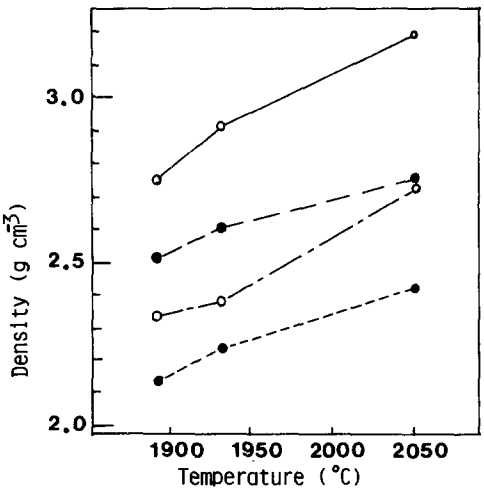

Figure 4 Densities of materials as a function of sintering temperature. Powder (– – –) A, (-----) B, (– – –) C, (——) D.

the solution–reprecipitation process. Microstructure development took place during the process, which determined the strength and fracture toughness of the sintered material. The requirement of high α content in the starting powder was to optimize the microstructure [9]. The reason that the powder characteristics do not influence the densification behaviour at $< 1800°$ C in the present study might be related to the smaller contribution of the phase-change process compared to pressureless sintering. The difference in the densification behaviour at $> 1800°$ C is not directly related to the α content in the starting powder because the α phase had transformed to β phase at $< 1800°$ C [6].

The densities of sintered materials and weight-loss values observed after sintering are shown in Figs 4 and 5, respectively. The materials with higher densities are obtained with smaller weight losses. A difference in density is related to that of the surface area [10], so a difference in weight loss might be attributed to that of the surface area of the sintered material. A weight loss is accompanied by the growth of pores from the surface of a compact [11], so a higher weight loss is

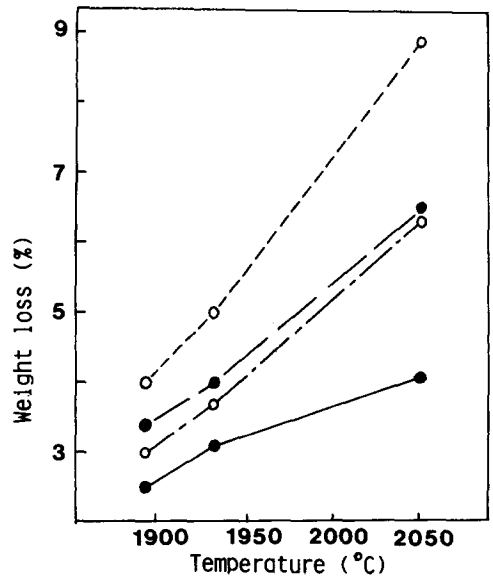

Figure 5 Weight loss observed after sintering. Powder (– – –) A, (-----) B, (– – –) C, (——) D.

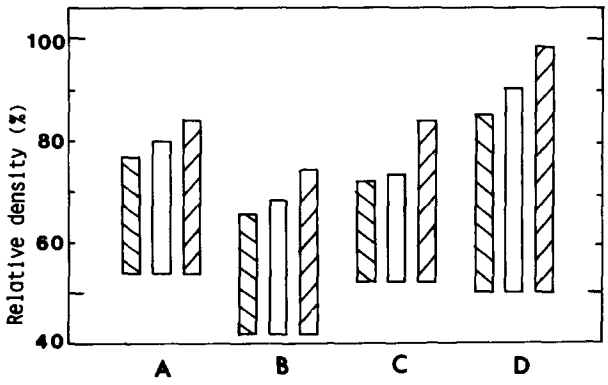

Figure 6 Relative densities of initial and sintered materials: ▨ 1890° C, □ 1930° C, ▨ 2050° C.

related to larger surface area and lower density. The relative densities of starting compacts and sintered materials are shown in Fig. 6.

The changes of density of materials as a function of temperature and heating time at 1930° C are shown in Fig. 7. The relations at 1890 and 2050° C are about the same as in Fig. 7. The sinterability is, of course, related to the final density of the sintered material, but it is easier to discuss it in terms of the initial density and the degree of shrinkage. Although the densification behaviour of Powder B is about the same as that of Powder D, the relation between the density and temperature or heating time is similar to that of Powders A and C as shown in Fig. 7. The main difference between Powders A, B and C is attributed to that of the initial density. Powder A has the highest initial density because of the wide range of particle size distribution. Powder B has the lowest initial density because of the presence of needle-like particles. Powder C is intermediate in density due to its uniform grain size. Powder A has the highest shrinkage rate at $< 1800°$ C as shown in Fig. 3. An analysis of grain boundary phases in sintered β-sialon with Y_2O_3 addition revealed that Powder A gave a higher SiO_2 concentration than Powder D [12]. The increased amount of SiO_2 at grain boundaries lowered the melting temperature and increased the amount of

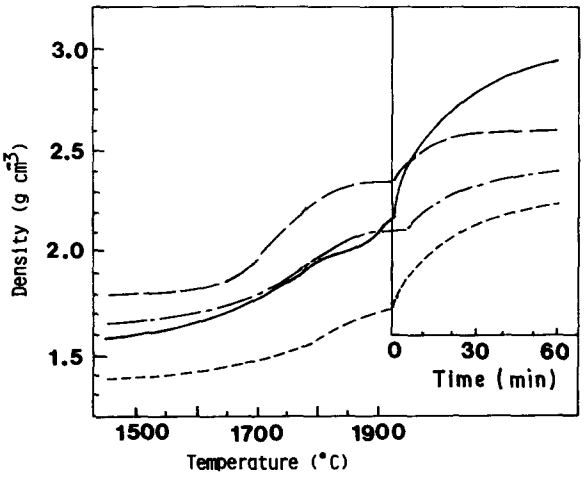

Figure 7 The change of density as a function of temperature and heating time at 1930° C. Powder (– – –) A, (-----) B, (– – –) C, (——) D.

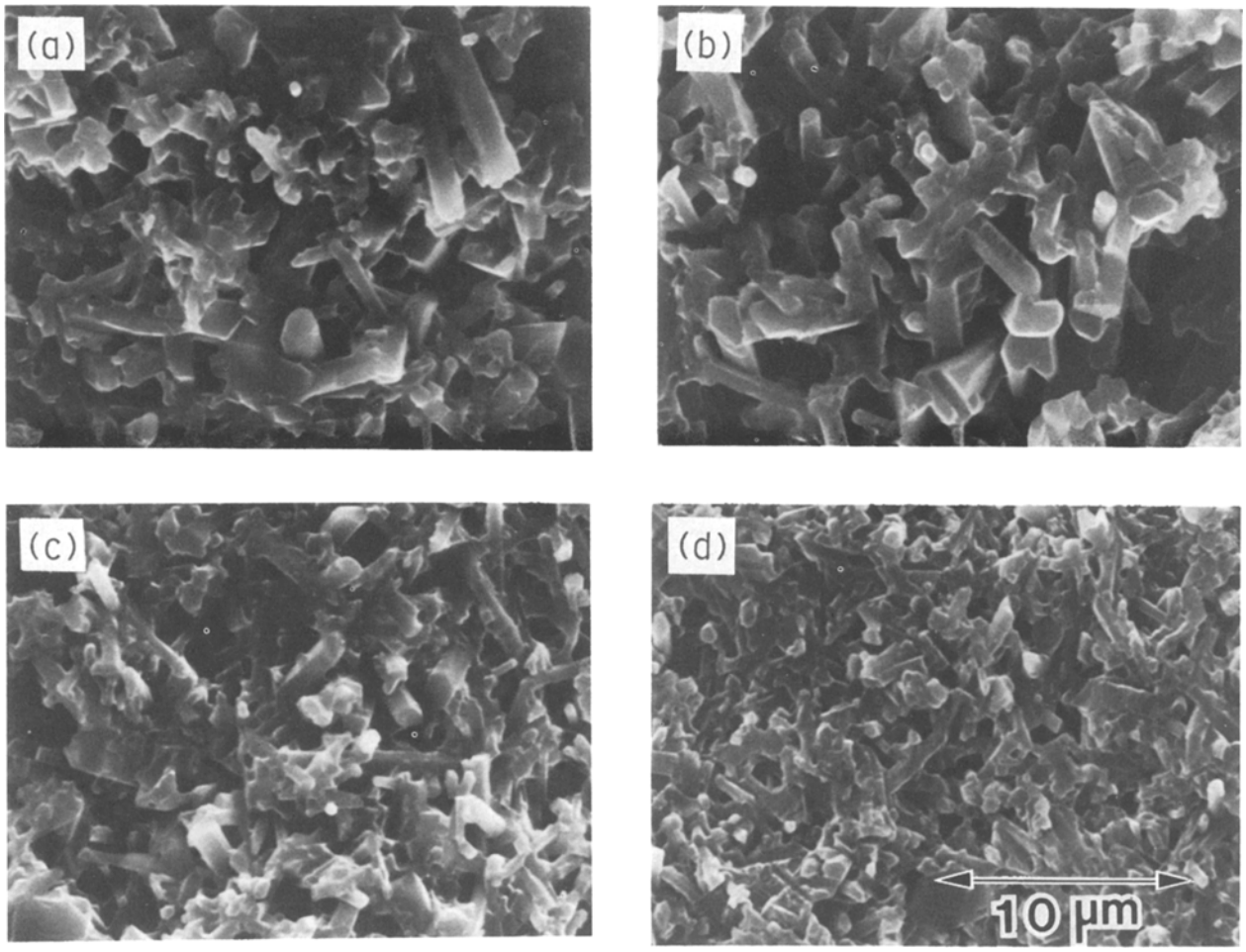

Figure 8 Fractured surfaces of materials fabricated at 1890° C from Powder (a) A, (b) B, (c) C and (d) D.

grain boundary phase so as to increase the shrinkage rate. The lowest density of material from Powder B might be related to the lowest initial density and the highest weight loss. It is most likely that the highest weight loss is related not only to the highest surface area but also to the presence of chlorine and OH in non-crystalline materials. Powder C showed a small shrinkage. The reason is attributed to the presence of carbon in the starting powder [1]. It is expected that the carbon is not free and is reacted as SiC because it was well burnt in an O_2 atmosphere. The reaction of SiC with SiO_2 forms SiO and CO at high temperature, which results in a decrease in the liquid phase. The presence of a small amount of liquid phase is responsible for the small shrinkage and grain growth during the sintering of Powder C.

Powder D gives the highest density due to the moderate initial density and highest shrinkage at $> 1800°$ C. The metallic compositions of the grain boundary phases in materials obtained at 1700 and 1930° C are shown in Table II [13]. The calculated values are based on the assumption that surface silica on the Si_3N_4 powder and Y_2O_3 did not dissolve into the grains, whereas 80 mol % of Al_2O_3 dissolved into the grains. The calculated and observed values are normalized by the yttrium content, because it is the most likely that all the Y_2O_3 remains at grain boundaries. The Si/Y and Al/Y ratios in materials obtained at 1700° C are not so different from the calculated values. This suggests that SiO_2 and Y_2O_3 remained at grain boundaries and that most of the Al_2O_3 dissolved into grains. The main composition of the grain boundary phase might be an oxide of the system SiO_2–Y_2O_3. i.e. $8.1SiO_2 \cdot 5Y_2O_3 \cdot 0.8Al_2O_3$. The grain boundary phases in materials obtained at 1930° C have higher silicon contents than those obtained at 1700° C. The aluminium content might be inferred to be the same as in materials at 1700° C because of the relatively large error in quantitative analysis due to the small amount. The result suggests that Si_3N_4 dissolved into the grain boundary phase at $> 1800°$ C. The composition should be $8.1SiO_2 \cdot 1.8Si_3N_4 \cdot 5Y_2O_3 \cdot 1.3Al_2O_3$. The calculated nitrogen content is 5.0 wt %. Although the presence of nitrogen in the grain boundary phase was not detected from the electron energy-loss spectrum (EELS), this may be due to the fact that the value is the same as the detection limit for nitrogen. The result reveals that the densification process observed at $> 1800°$ C is due to the diffusion of material through the increased amount of liquid phase. It is expected

TABLE II Metallic composition of grain boundary phase in sintered materials from Powder D

Sintering temperature (° C)	Metallic composition (at %)		
	Y	Si (Si/Y)	Al (Al/Y)
1700	50.6	41.0 (0.81)	8.3 (0.16)
1930	38.5	51.6 (1.34)	9.9 (0.26)
Calculated	55.4	34.8 (0.63)	9.8 (0.18)

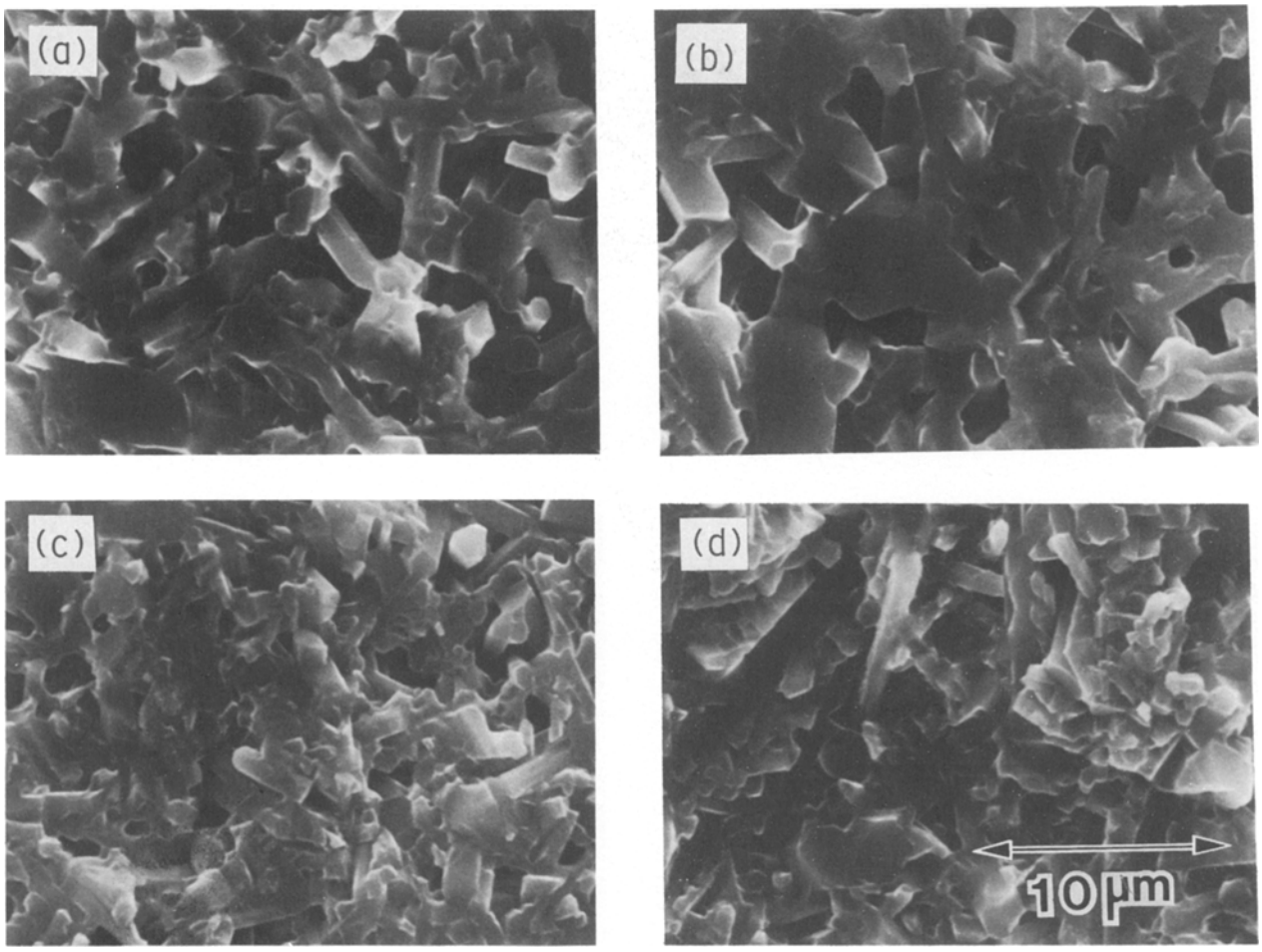

Figure 9 Fractured surfaces of materials fabricated at 2050° C from Powder (a) A, (b) B, (c) C and (d) D.

that the same reaction to increase the amount of grain boundary phase may occur in materials from Powders A and B, but the contribution of the high-temperature process is small because of the elongation of grains at low temperature as shown below.

The fractured surfaces of materials obtained at 1890 and 2050° C are shown in Figs 8 and 9, respectively. Fig. 9d shows that the densification at $> 1800°$ C is accompanied by the growth of needle-like β-Si_3N_4 grains in an equi-axial β-Si_3N_4 matrix. The fracture toughness of sintered material is increased by this "composite" microstructure. The increase in fracture toughness is related to the increase in the aspect ratio of needle-like grains [7, 8, 14]. The growth of needle-like grains is also detected in Figs 8a and b, where the relative density is fairly low compared to that of materials from Powder D. The solution–reprecipitation at $< 1800°$ C is based on the dissolution of small grains and overgrowth on large grains. The grain growth was accelerated by the size distribution [12]. The presence of larger amounts of SiO_2 in Powders A and B might also be responsible for the grain growth. Sinterability is destroyed by the grain growth. The grain growth is also accompanied by the growth of pores as shown in Figs 9a and b. There is a critical pore radius over which pores do not shrink by sintering [15]. This might be the reason why Powders A and B did not densify appreciably at $> 1800°$ C.

Brook *et al.* [16] discussed the sinterability of ceramic powders and the effect of additives in terms of the ratio of grain growth to densification. They defined the factor

$$\Gamma^* = \frac{\text{Grain growth rate}}{\text{Densification rate}} = \frac{\dot{G}\varrho}{G\dot{\varrho}} \quad (1)$$

Where G and $\dot{G}$ are the grain size and rate of grain growth, respectively. ϱ and $\dot{\varrho}$ are the density and the rate of densification, respectively. They observed that additives for Al_2O_3 sintering decreased the Γ^* factor in the high relative density region, which increased the final density. Bellosi *et al.* [3] observed the Γ^* factor in the pressureless sintering of Si_3N_4. They revealed that the difference in Γ^* due to a difference in powder characteristics was small at 85% relative density, but it was large at 90% relative density. They attributed the difference in Γ^* to that of the viscosity of the liquid phase and the resultant microstructure.

In the present study, the shrinkage rate at a constant heating rate is obtained from Fig. 2. The relation between the density and grain growth was compared in Powders A and D. Powder A was a representative of the group of Powders A, B and C. The rate of grain growth during sintering of Powder A is larger than that of Powder D. Appreciable grain growth is observed at 70 to 80% relative density for Powder A, whereas it is not observed at 85% relative density for Powder D. For the evaluation of sinterability, the F factor is defined in present study:

$$F = k\dot{l}/\dot{g} \quad (2)$$

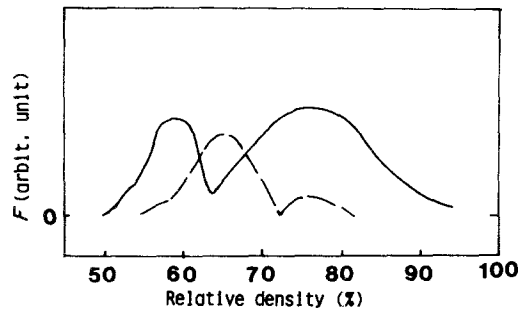

Figure 10 Plot of F factor as a function of relative density for Powder (– – –) A, (——) D.

where k is a constant, $\dot{l}$ is the rate of linear shrinkage and $\dot{g}$ is the rate of grain growth. A qualitative representation of F is shown in Fig. 10 as a function of relative density. It is shown that Powder D had a higher F value at high relative density. This shows that the abnormal grain growth in materials from Powder A at low relative density retarded further densification. The growth of needle-like grains may occur when grains are covered with liquid phase completely and have enough space around the grains. The fact that needle-like grains are observed at low relative density in materials from Powder A suggests that there is a large inhomogeneity in the compacts. The large size distribution may be responsible for the local distribution of liquid phase. The growth of needle-like grains at low relative density results in the growth of pores and the retardation of further densification. On the other hand, the compacts from Powder D keep a uniform microstructure over a wide range of relative density. A uniform distribution of small pores retards the growth of needle-like grains at low relative density. The growth of needle-like grains is observed only when the relative density exceeds about 85%. It was concluded that it is necessary to keep the microstructure uniform up to about 1800° C to get high-density materials by gas pressure sintering.

4. Conclusions

A desirable powder for gas pressure sintering of Si_3N_4 with 5 wt % Y_2O_3 and 2 wt % Al_2O_3 addition should have the following properties:

1. High purity in terms of metallic and non-metallic impurities. The presence of impurities lowers the melting temperature of liquid phase which increases the rate of grain growth.
2. Spherical particles to give uniform and high-density compacts.
3. A narrow size distribution to minimize the grain growth at $< 1800°$ C and at low relative density.

If the conditions are fulfilled, densification at $< 1800°$ C should not accompany appreciable grain growth. Densification at $> 1800°$ C through the increased amount of liquid phase should contribute to further densification. The growth of needle-like grains in a uniform matrix at the final stage of densification would give sintered materials with "composite" microstructures and high fracture toughness.

References

1. G. WÖTTING and G. ZIEGLER, *Ceram. Int.* **10** (1984) 18.
2. K. HOMMA, H. OKADA and T. TATSUNO, *Yogyo-Kyokai-Shi* **95** (1987) 323.
3. A. BELLOSI, C. GALASSI and D. D. FABBRICHE, in "Proceedings of International Conference on High Temperature and Energy-Related Materials, Rome, 1987), to be published.
4. R. E. LOEHMAN and D. J. ROWCLIFFE, *J. Amer. Ceram. Soc.* **63** (1980) 144.
5. A. TSUGE and K. NISHIDA, *Amer. Ceram. Soc. Bull.* **57** (1978) 424.
6. M. MITOMO, *J. Mater. Sci.* **11** (1976) 1103.
7. M. MITOMO and K. MIZUNO, in "Ceramic Materials and Components for Engines", edited by W. Bunk and H. Hausner (German Ceramic Society, Bad Honnet, Germany, 1986) p. 263.
8. K. T. FABER and A. G. EVANS, *Acta Metall.* **31** (1983) 577.
9. F. F. LANGE, *J. Amer. Ceram. Soc.* **62** (1979) 428.
10. C. GRESKOVICH and J. M. ROSOLOWSKI, *ibid.* **59** (1976) 336.
11. G. R. TERWILLIGER and F. F. LANGE, *J. Mater. Sci.* **10** (1975) 1169.
12. Y. BANDO, M. MITOMO and Y. KITAMI, *J. Electron Microsc.* **35** (1986) 371.
13. Y. BANDO, N. NOGAMI and M. MITOMO, to be published.
14. E. TANI, S. UMEBAYASHI, K. KISHI, K. KOBAYASHI and M. NISHIJIMA, *J. Mater. Sci.* **4** (1984) 1454.
15. M. MITOMO, N. NAGATA and M. TSUTSUMI, in Proceedings of First International Symposium on Ceramic Components for Engines, Hakone, Japan, edited by S. Somiya, E. Kanai and K. Ando (KTK Science Publishers, Tokyo, Japan, 1983) p. 31.
16. R. J. BROOK, E. GILBART, N. J. SHAW and U. EISELE, *Powder Metall.* **28** (1985) 105.

Received 15 September 1987
and accepted 19 January 1988